AN793

Power Management in Portable Applications: Understanding the Buck Switchmode Power Converter

Author: *Scott Dearborn*
Microchip Technology Inc.

INTRODUCTION

Powering today's portable world poses many challenges for system designers. The use of batteries as a prime power source is on the rise. As a result, a burden has been placed on the system designer to create sophisticated systems utilizing the batteries full potential.

Each application is unique, but one common theme rings through: ***maximize battery capacity usage***. This theme directly relates to how efficiently the energy from the batteries is converted and transferred to the system load. No single method is ideal for all applications. Linear regulators, switched capacitor charge pumps, and inductor based switchmode power converters are all employed. Each method has its associated advantages and disadvantages. It is the particular application with its individual requirements that determines which method will be the best to use.

This application note focuses on the fundamentals of inductor based switchmode power converters. This is a "grass roots" approach to understanding switchmode power converters. Specifically, the basic buck circuit topology and its associated waveforms will be examined both empirically and mathematically.

All known switchmode power converters can be derived from combinations of the basic buck and / or boost converters along with some form of transformation function. Roughly 85% of today's switchmode power converters are derived from the buck topology. Understanding its operation is essential to switchmode power converter design.

SWITCHMODE POWER CONVERTER

The simplest form of a switchmode power converter is illustrated in Figure 1. The ideal switch opens and closes at a frequency of 1/T, where T represents the switch cycle period. The ratio of the on-time, or conduction time of the switch, to the period is referred to as the duty cycle, D.

$$D \equiv \frac{t_{ON}}{T}$$

The resulting load voltage, V_O, is a chopped version of the input. The load voltage looks like a series of pulses having an amplitude equal to the source voltage, V_S. The average, or DC, value of the load voltage is simply the source voltage multiplied by the duty cycle.

$$V_{O(AVG)} = V_S \times D$$

In this simple configuration, the load voltage is always less than or equal to the source voltage with the same polarity. The DC load voltage does not come without a price. Substantial ripple is present not only in the load voltage, but in the input source current as well. Most applications can not take advantage of this type of conversion without employing some type of low pass filter to smooth the ripple.

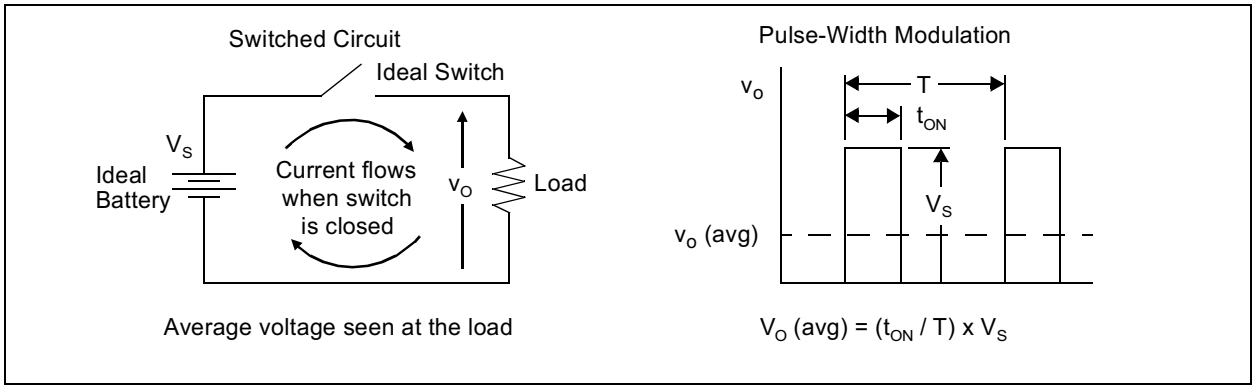

FIGURE 1: *Simplest form of a switchmode power converter*

© 2001 Microchip Technology Inc.

BASIC BUCK TOPOLOGY

By inserting a low pass filter between the switch and the load, a basic buck topology is formed. As a result, the buck converter (as the name implies) "bucks" or chops the input source voltage to a lower magnitude load voltage.

Figure 2A depicts the idealized buck converter. The single pole double throw switch alternates between positions 1 and 2. Figures 2B and 2C depict the switch in each state. A practical realization of the ideal buck topology is illustrated in Figure 2D.

During a switch cycle, the switch transitions between positions 1 and 2. If a switch cycle begins in position 1, the voltage across the inductor, L, is equal to the source voltage, V_S, minus the load voltage, V_O. At the end of the on-time, t_{ON}, the switch changes to position 2. The voltage across the inductor collapses, changing polarity to a value equal to $-V_O$. The switch remains off until the end of the period when the switch returns to position 1 completing the cycle.

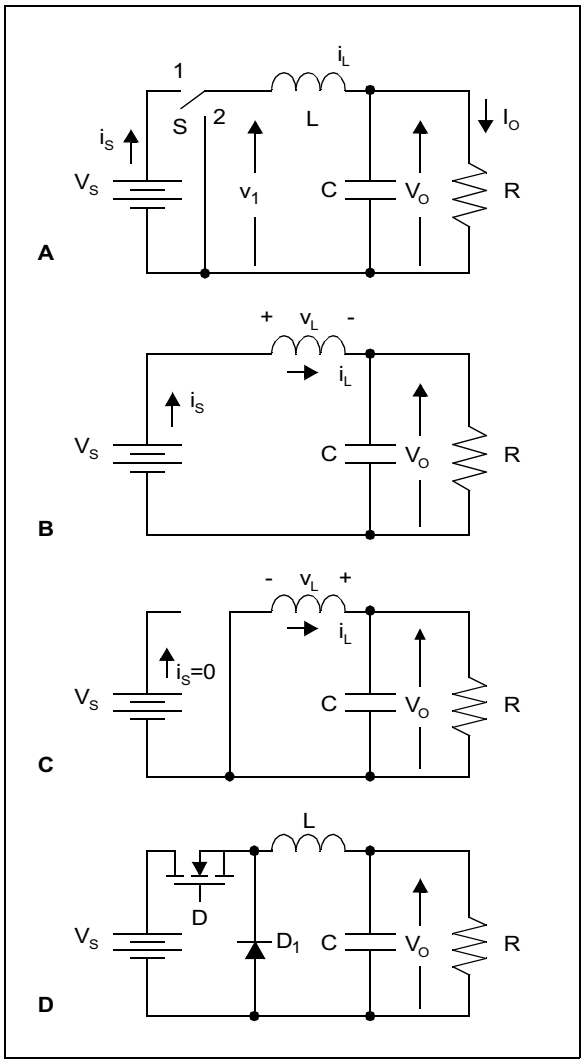

FIGURE 2: *Ideal Buck Topology*

Two scenarios are possible at the end of the cycle. The first scenario occurs when all the energy stored in the inductor has been transferred to the load, i_L equals zero. This is known as ***discontinuous mode*** of operation. The second scenario occurs when current continues to flow at the end of the cycle, i_L equals some non-zero value. This is known as ***continuous mode*** of operation. The inductor current conduction mode plays an important role in determining the conversion characteristics and circuit performance.

For fixed values of L and D, the mode in which the converter operates is determined by the load, R. As the load increases in ohmic value, the operating mode will change from continuous to discontinuous. Also, the inductor value needed to maintain continuos mode operation is directly proportional to the switch cycle period. It is often desirable to operate a buck converter only in the continuous mode. We will examine both modes of operation in detail to get a better understanding of why this would be desirable.

But first lets step back and look at the pieces of the buck topology. As stated previously, the buck topology is a simple converter followed by a low pass LC filter. By examining the circuit, we can see that V_O is the average value of v_1. Voltage v_1 consists of both AC and DC components. Since the average or DC value is desired, the LC filter must sufficiently remove the unwanted AC components. This implies that the corner frequency of the filter must be much less than the switching frequency.

$$1/T > 1/(2\pi\sqrt{LC})$$

Intuition tells us that a value for L can be chosen to maintain continuous mode operation and C can then be chosen to produce the desired amount of filtering. However, capacitors are not pure reactive devices and as a result contain some equivalent series resistance, ESR, that produces unwanted output voltage ripple in conjunction with the inductor current ripple. A trade-off must be made between inductor and capacitor values in order to produce the desired performance. The following discussion will assume that the LC filter components have been chosen adequately to remove the AC components and the load will be considered DC.

Continuous Mode Operation

As was eluded to earlier, it is often desirable to operate a buck converter in the continuous mode. Figure 3 depicts the circuit used to analyze both modes of operation. An input filter network has been inserted to minimize the input current ripple so that I_S can be considered essentially DC. Figure 4 depicts the waveforms associated with continuous mode operation. Ideal circuit elements will be examined to mathematically derive a steady-state large signal representation of the circuit. However, parasitic elements can easily be inserted into the mathematical models to represent

© 2001 Microchip Technology Inc.

non-ideal characteristics of real circuit components, such as inductor winding resistance or filter capacitor ESR. Despite this limited approach, the models still have more than adequate accuracy for practical design purposes.

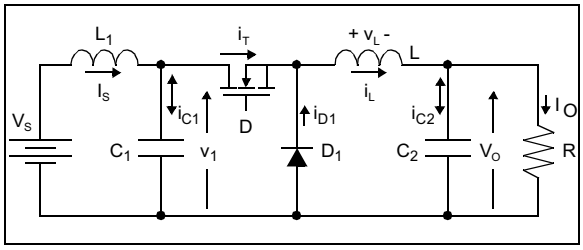

FIGURE 3: *Circuit used to analyze modes of operation*

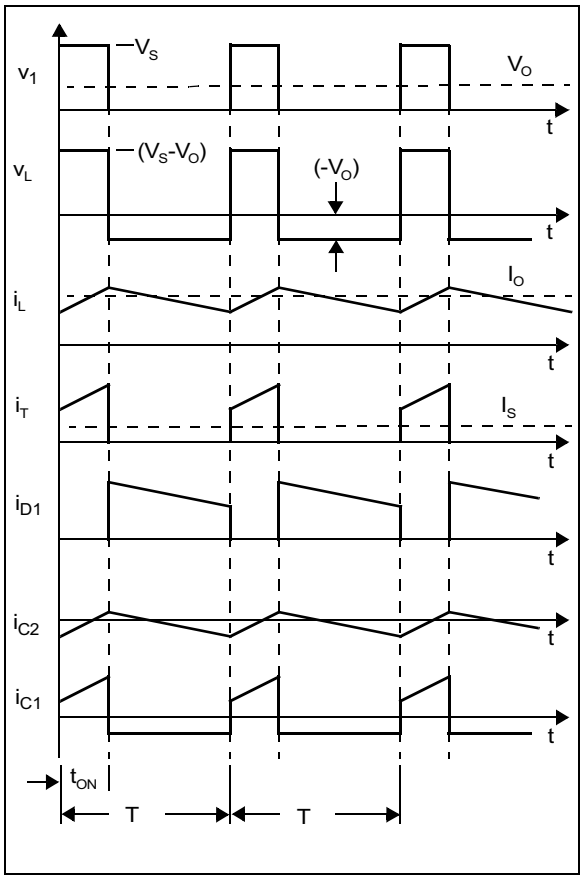

FIGURE 4: *Continuous mode waveforms*

The examination will start with the inductor, L. An ideal inductor is an energy storage element that can not support a non-zero average voltage. In other words, the volt-time product of each switch state must be equal in steady-state operation.

$$\frac{1}{T}\times\left[\int_{O}^{t_{ON}}(V_s - V_O)dt + \int_{t_{ON}}^{T}(-V_O)dt\right] = 0$$

$$(V_S - V_O)\times t_{ON} = V_O\times(T - t_{ON})$$

Rearranging the equation we get:

$$\frac{t_{ON}}{T} = \frac{V_O}{V_S}$$

From this equation, we determine that the switch duty cycle is independent of the circuit elements and is equal to the input-to-output DC transfer function, M.

$$M \equiv \frac{V_O}{V_S}$$

Further examination of the circuit tells us that the average inductor current is equal to the DC load current.

$$i_{L(AVG)} = \frac{Ia + Ib}{2} = \frac{V_O}{R}$$

Where Ia is the minimum inductor current and Ib is the maximum inductor current.

$$Ia = Ib - \frac{V_O}{L}\times(T - t_{ON})$$

$$Ib = Ia + \frac{V_S - V_O}{L}\times t_{ON}$$

At this point, it is desirable to define the normalized inductor time constant and solve for Ia and Ib. The normalized inductor time constant is:

$$\tau_L \equiv \frac{L}{R\times T}$$

Solving for Ia and Ib, with the constraints of $i_{L(AVG)}$, in terms of the normalized inductor time constant and the DC transfer function, produces the following results:

$$Ia = \frac{V_O}{R}\times\left[1 - \frac{1-M}{2\times\tau_L}\right]$$

$$Ib = \frac{V_O}{R}\times\left[1 + \frac{1-M}{2\times\tau_L}\right]$$

The switch conducts current only during the on-time. The switch current, represented by i_T, can be approximated by a trapezoid. The switch turns on and immediately takes over the current flow into the inductor at an amplitude equal to Ia. The current ramps to a final value equal to Ib. The average and RMS current values will be that of the trapezoid waveform referenced in Appendix A. Also, the average value of the switch current is equal to the average value of the source current.

The average value of the switch current will be:

$$i_{T(AVG)} = \frac{t_{ON} \times (Ia + Ib)}{T \times 2} = \frac{M \times V_O}{R}$$

The RMS value of the switch current will be in the following form.

$$i_{T(RMS)} = \sqrt{\frac{t_{ON} \times (Ia^2 + Ia \times Ib + Ib^2)}{T \times 3}}$$

Substituting for Ia and Ib yields:

$$i_{T(RMS)} = \frac{V_O}{R} \times \sqrt{M \times \left[1 + \frac{1}{12}\left(\frac{1-M}{2 \times \tau_L}\right)^2\right]}$$

The diode, D_1, conducts current only during the time when the switch is off. The diode current, represented by i_{D1}, can also be approximated by a trapezoid. The diode begins conducting current at an amplitude equal to Ib. The current ramps down to a final value equal to Ia. The average and RMS current values will be that of the trapezoid waveform.

The average value of the diode current will be:

$$i_{D1(AVG)} = \frac{(T - t_{ON}) \times (Ia + Ib)}{T \times 2} = \frac{(1-M) \times V_O}{R}$$

The RMS value of the diode current will be:

$$i_{D1(RMS)} = \frac{V_O}{R} \times \sqrt{(1-M) \times \left[1 + \frac{1}{12}\left(\frac{1-M}{2 \times \tau_L}\right)^2\right]}$$

The ripple current in the inductor can be used to determine the RMS current in the output capacitor. Based on our assumption that our LC filter is adequate, the AC component of the inductor current will flow into C_2 and not into the load.

$$i_{C2(RMS)} = \frac{(Ib - Ia)}{\sqrt{12}}$$

Substituting for Ib and Ia gives:

$$i_{C2(RMS)} = \frac{V_O}{R} \times \left[\frac{1-M}{\sqrt{12} \times \tau_L}\right]$$

The input capacitor RMS current will take on the form shown below:

$$i_{C1(RMS)} = \sqrt{M \times \left[\frac{Ia^2 + IaIb + Ib^2}{3} - \frac{M}{4}(Ia + Ib)^2\right]}$$

Again, substituting for Ib and Ia gives:

$$i_{C1(RMS)} = \frac{V_O}{R} \times \sqrt{M \times \left[(1-M) + \frac{1}{12}\left(\frac{1-M}{2 \times \tau_L}\right)^2\right]}$$

The root of the second term is generally small in comparison to the first term, so the input capacitor RMS can be approximated by:

$$i_{C1(RMS)} = \frac{V_O}{R} \times \sqrt{M - M^2}$$

As a rule of thumb, the RMS current of the input filter capacitor can be approximated to be one half the DC load current. Careful attention should be paid to the currents found in the filter capacitors. The high ripple currents in the filter capacitors cause internal heat build up which could cause erratic operation or premature destruction of the devices.

Discontinuous Mode Operation

Hopefully now the waveforms of the continuous mode of operation are more clearly understood. Our attention will now shift to the discontinuous mode of operation. Although it is desirable to operate a buck converter in the continuous mode, this goal is not always achievable when dealing with a wide variation in load currents or input voltages. At some point, the mode of operation will shift to discontinuous, unless some means of pulse frequency modulation is employed. The waveforms associated with the discontinuous mode of operation are shown in Figure 5.

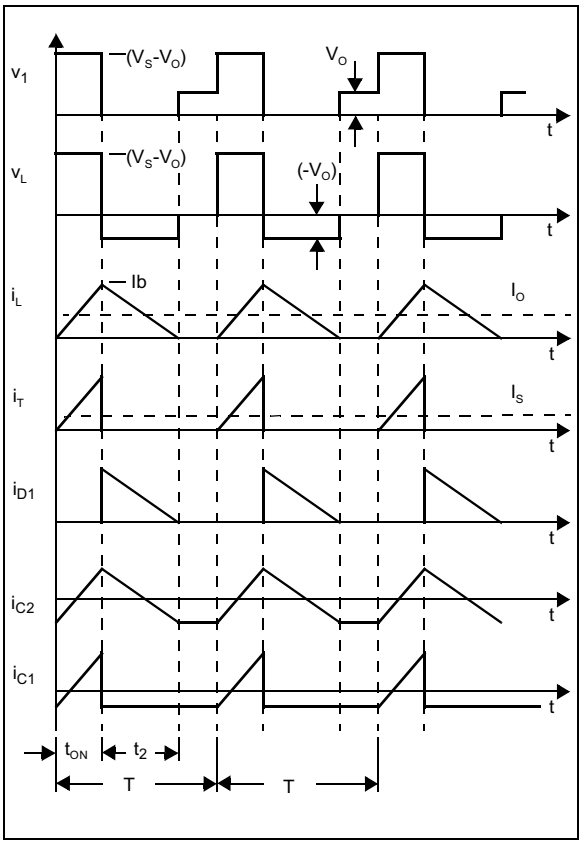

FIGURE 5: *Discontinuous mode waveforms*

© 2001 Microchip Technology Inc.

Again, our examination will start with the inductor. As stated previously, the average voltage across the inductor must be equal to zero.

$$\frac{1}{T}\times\left[\int_0^{t_{ON}}(V_S-V_O)dt+\int_{t_{ON}}^{t_2}(-V_O)dt+\int_{t_2}^{T}0dt\right]=0$$

$$(V_S-V_O)\times t_{ON}=V_O\times t_2$$

Where t_2 is the time from when the switch opens to when the inductor current reaches zero.

By definition, the minimum inductor current, Ia, equals zero. The maximum inductor current, Ib, can be found in terms of the switch on-time.

$$V=L\times\frac{di}{dt}$$

Knowing the initial value of the inductor current is zero, this equation can be rearranged to find the maximum current.

$$Ib=\frac{V_S-V_O}{L}\times t_{ON}$$

As with the continuous mode, the average, or DC, value of the inductor current is equal to the load current. The average current of the inductor takes on the form:

$$i_{L(AVG)}=\frac{Ib\times(t_{ON}+t_2)}{2\times T}=\frac{V_O}{R}$$

Substituting for Ib and t_2 yields a switch duty cycle equal to:

$$\frac{t_{ON}}{T}=M\times\sqrt{\frac{2\times\tau_L}{1-M}}$$

This equation indicates that the switch duty cycle in discontinuous mode is dependant on the inductor value, DC transfer function, and load current. Also from this equation, we can see that the boundary between continuous mode and discontinuous mode occurs where the normalized inductor time constant equals one-half one minus the DC transfer function.

$$\tau_{LC}=\frac{1-M}{2}$$

The peak inductor current can be expressed in terms of the normalized inductor time constant and the DC transfer function.

$$Ib=\frac{V_O}{R}\times\sqrt{\frac{2\times(1-M)}{\tau_L}}$$

As with continuous mode, the switch conducts current only during the on-time. The switch current, represented by i_T, can be approximated by a triangular waveform. The switch turns on and starts ramping current up in the inductor from zero. The current ramps to a final value equal to Ib. The average and RMS current values will be that of the triangular waveform. Again, the average value of the switch current is equal to the average value of the source current.

The average value of the switch current will be:

$$i_{T(AVG)}=\frac{t_{ON}\times Ib}{T\times 2}=\frac{M\times V_O}{R}$$

The RMS value of the switch current will be in the following form.

$$i_{T(RMS)}=Ib\times\sqrt{\frac{t_{ON}}{T\times 3}}$$

Substituting for Ib yields:

$$i_{T(RMS)}=\frac{V_O}{R}\times\left(\frac{8}{9}\times M^2\times\left[\frac{1-M}{\tau_L}\right]\right)^{\frac{1}{4}}$$

The diode, D_1, conducts current from when the switch is turned off until the inductor current has diminished to zero. The diode current, represented by i_{D1}, can also be approximated by a triangular waveform. The diode begins conducting current at an amplitude equal to Ib. The current ramps down to a final value equal to zero. The average and RMS current values will be that of the triangular waveform.

The average value of the diode current will be:

$$i_{D1(AVG)}=\frac{V_O}{R}\times\sqrt{2\times\tau_L\times(1-M)}$$

The RMS value of the diode current will be:

$$i_{D1(RMS)}=\frac{V_O}{R}\times\left(\frac{8}{9}\times\left[\frac{(1-M)^3}{\tau_L}\right]\right)^{\frac{1}{4}}$$

The RMS ripple current in the output capacitor is then derived to be:

$$i_{C2(RMS)}=\frac{V_O}{R}\times\left[\sqrt{\frac{8}{9}\times\frac{1-M}{\tau_L}-1}\right]^{\frac{1}{2}}$$

And the RMS ripple current for the input capacitor is derived to be:

$$i_{C1(RMS)}=\frac{V_O}{R}\times\left[\sqrt{\frac{8}{9}\times\frac{1-M}{\tau_L}-M^2}\right]^{\frac{1}{2}}$$

© 2001 Microchip Technology Inc.

Table 1 summarizes the circuit characteristics for both modes of operation.

TABLE 1: *Characteristic Summary*

Variable Description	Variable	Continuous Mode	Discontinuous Mode
Input-to-Output DC Transfer Function	M	$\frac{V_O}{V_S}$	$\frac{V_O}{V_S}$
Normalized Inductor Time Constant	τ_L	$\frac{L}{R \times T}$	$\frac{L}{R \times T}$
Switch Conduction Duty Cycle	D	M	$M \times \sqrt{\frac{2 \times \tau_L}{1 - M}}$
Minimum Inductor Current	Ia	$\frac{V_O}{R} \times \left[1 - \frac{1 - M}{2 \times \tau_L}\right]$	0
Maximum Inductor Current	Ib	$\frac{V_O}{R} \times \left[1 + \frac{1 - M}{2 \times \tau_L}\right]$	$\frac{V_O}{R} \times \sqrt{\frac{2 \times (1 - M)}{\tau_L}}$
Average Inductor Current	$i_{L(AVG)}$	$\frac{V_O}{R}$	$\frac{V_O}{R}$
Average Switch Current	$i_{T(AVG)}$	$\frac{M \times V_O}{R}$	$\frac{M \times V_O}{R}$
RMS Switch Current	$i_{T(RMS)}$	$\frac{V_O}{R} \times \sqrt{M \times \left[1 + \frac{1}{12}\left(\frac{1 - M}{2 \times \tau_L}\right)^2\right]}$	$\frac{V_O}{R} \times \left(\frac{8}{9} \times M^2 \times \left[\frac{1 - M}{\tau_L}\right]\right)^{\frac{1}{4}}$
Average Diode Current	$i_{D1(AVG)}$	$\frac{(1 - M) \times V_O}{R}$	$\frac{V_O}{R} \times \sqrt{2 \times \tau_L \times (1 - M)}$
RMS Diode Current	$i_{D1(RMS)}$	$\frac{V_O}{R} \times \sqrt{(1 - M) \times \left[1 + \frac{1}{12}\left(\frac{1 - M}{2 \times \tau_L}\right)^2\right]}$	$\frac{V_O}{R} \times \left(\frac{8}{9} \times \left[\frac{(1 - M)^3}{\tau_L}\right]\right)^{\frac{1}{4}}$
Input Capacitor Ripple Current	$i_{C1(RMS)}$	$\frac{V_O}{R} \times \sqrt{M\left[(1 - M) + \frac{1}{12}\left(\frac{1 - M}{2 \times \tau_L}\right)^2\right]}$	$\frac{V_O}{R} \times \left[\sqrt{\frac{8}{9} \times \frac{1 - M}{\tau_L}} - M^2\right]^{\frac{1}{2}}$
Output Capacitor Ripple Current	$i_{C2(RMS)}$	$\frac{V_O}{R} \times \left[\frac{1 - M}{\sqrt{12} \times \tau_L}\right]$	$\frac{V_O}{R} \times \left[\sqrt{\frac{8}{9} \times \frac{1 - M}{\tau_L}} - 1\right]^{\frac{1}{2}}$
Average Input Source Current	$I_{S(AVG)}$	$\frac{M \times V_O}{R}$	$\frac{M \times V_O}{R}$

© 2001 Microchip Technology Inc.

Continuous versus Discontinuous

So why is continuous mode preferred? As can be seen by examining the waveforms and the mathematical models, the peak current stresses on the circuit elements will always be less in continuous mode for a given set of input and output conditions. The peak-to-peak inductor current ripple is always less in continuous mode for a given set of input and output conditions. This directly corresponds to load voltage ripple and stress placed on the filter components. Although the input current to the converter is always pulsing, output current pulses are much more controlled in continuous mode.

Most applications are designed to be well beyond the continuous-discontinuous boundary when operating at full load. Some applications may transition into discontinuous mode at light loads. This, however, generally does not pose a problem to the system because stress levels have been substantially reduced.

DESIGN EXAMPLE

A practical design example will be presented along with actual continuous mode and discontinuous mode waveforms for comparison to the ideal situation of the preceding discussion.

The design parameters are given as follows:

Input Source:	Single cell Lithium-Ion
Load Voltage:	3.0V
Load Voltage Ripple:	1% peak-to-peak
Minimum Load Current:	10 µA
Maximum Load Current:	250 mA

A Microchip TC105303ECT was chosen as the control IC setting the switching frequency to 300 kHz.

Figure 6 illustrates the practical design schematic.The component values represent those chosen with the TC105303 controlling the time sampled switching. Node v_1 is a test point corresponding to the v_1 waveforms from Figures 4 and 5.

Component Selection

Inductor

Now, as with the ideal analysis, the design will start with the inductor. As a rule of thumb, a good starting point is to choose an inductor value producing a maximum peak-to-peak ripple current equal to ten percent of the maximum load current. This will limit the RMS current in the output filter capacitor and, as a second order effect, keep the core losses in the inductor reasonable. The maximum peak-to-peak ripple current will occur when the input source voltage is at its maximum potential. For this application with a single cell lithium-ion battery as the source, the maximum voltage will be 4.2V.

$$V = L \times \frac{di}{dt}$$

$$L = V_S - V_O \times \frac{M \times T}{I_O \times 0.10}$$

$$L = (4.2 - 3.0) \times \frac{\left(\frac{3.0}{4.2}\right) \times \frac{1}{300K}}{0.250 \times 0.10} \approx 100\mu H$$

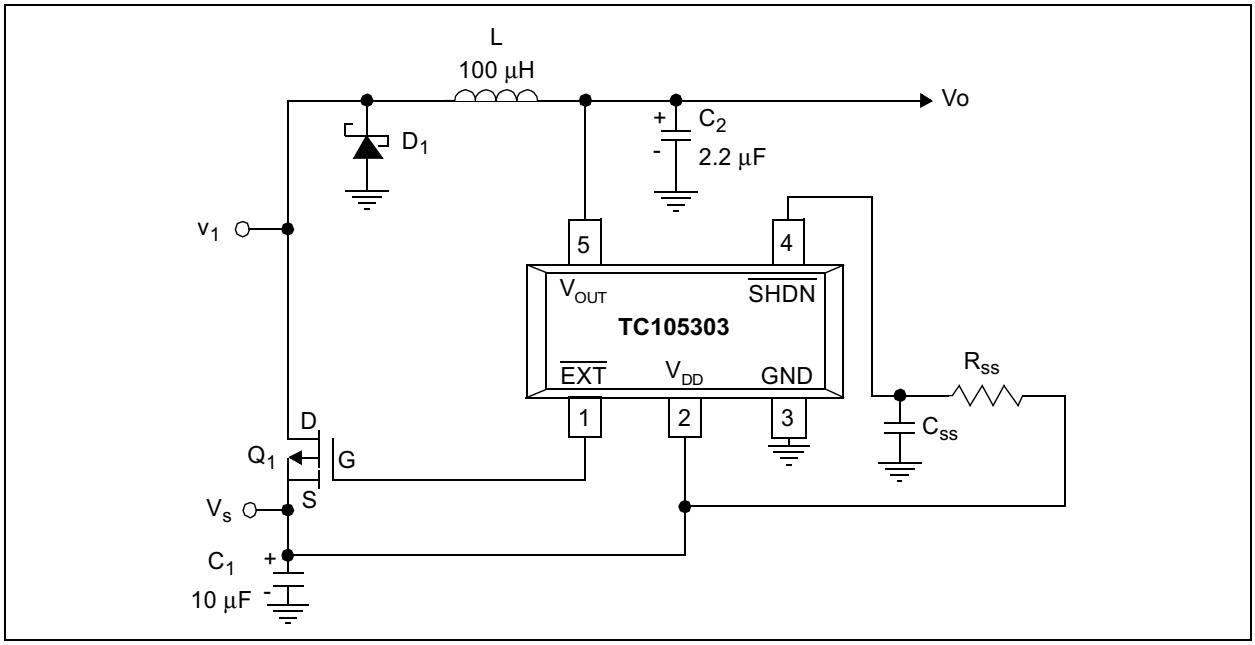

FIGURE 6: *Buck circuit realization*

The inductor must be selected to handle both peak and RMS currents. In addition, winding resistance losses can become significant at higher output currents reducing the systems efficiency.

Load Filter Capacitor

The next circuit element to choose is the load filter capacitor. As another rule of thumb, a good starting point is to set the filter characteristic impedance equal to the load resistance.This will produce a voltage overshoot of the square root of two times the load voltage if the converter is operating at full rated load and the load is abruptly removed.

$$Z_O \equiv \sqrt{\frac{L}{C}}$$

$$C = \frac{L}{R^2} = \frac{I_O^2 \times L}{V_O^2} = \frac{0.250^2 \times 100 \times 10^{-6}}{3.0^2} \approx 1\mu F$$

To verify the capacitor value, the load ripple voltage is checked.The ripple voltage due to the capacitance is:

$$\Delta v = \frac{1}{C} \times \int_0^{t_{ON}} i(t)dt = \frac{1}{C} \times \int_0^{t_{ON}} \frac{V_S - V_O}{L} \times tdt$$

$$\Delta v = \frac{1}{1 \times 10^{-6}} \times \frac{4.2 - 3.0}{100 \times 10^{-6}} \times \frac{t^2}{2}\Bigg|_0^{t_{ON}} \approx 34mV$$

The ripple voltage exceeds the design parameter of 1% peak-to-peak output voltage ripple. Therefore, the output capacitor will be increased to 2.2 µF. This produces an output voltage ripple of 15.5 mV and leaves about 14.5 mV of ripple due to capacitor ESR and for design margin. For now, we will assume this value will work and produce adequate results. Of course, now is the time to conduct design trade-off studies and experiment with different combinations of L's and C's. The values can be changed to reduce cost, size, or weight to meet the needs of the particular application. These values should suffice for our needs.

A second check of the capacitor value is the corner frequency of the LC filter. As mentioned in the preceding discussion, the filter capacitor corner frequency should be much lower than the switching frequency. Usually an order of magnitude or better is required to minimize the load voltage ripple.

$$f_C = \frac{1}{2 \times \pi \times \sqrt{L \times C}} = \frac{1}{2 \times \pi \times \sqrt{100 \times 10^{-6} \times 10^{-6}}}$$

$$f_C \approx 10.7kHz$$

This concurs with our earlier conclusions, so this is the value we will use for evaluation.

The capacitance value alone is not enough. The capacitor must be able to handle the worst case RMS current and have the proper voltage rating.

Switch and Catch Diode

The switch and catch diode were chosen based on voltage and current rating. The switch, a P-channel MOSFET, ideally sees a worst case source-to-drain voltage of the maximum input source voltage plus the forward voltage drop of the catch diode. The catch diode sees a worst case reverse voltage equal to the maximum source voltage.

A trade-off must be made between the switch on-resistance, gate charge, gate threshold, and physical size to reduce both switching and conduction losses.

Input Filter Capacitor

The input capacitor is essential to the proper operation of the circuit. The input capacitor is chosen by its RMS current rating and voltage rating. The input filter inductor was omitted from this design. However, some inductance may be required in certain applications. The AC component of the input current can radiate noise to adjacent circuitry. A small amount of inductance between the input source and input filter capacitor can greatly isolate and attenuate the noise. Care should be taken when adding impedance to the source. An inappropriate amount of impedance can cause loop instability and erratic operation.

Continuous Mode Validation

In order to verify the mathematical models, the circuit in Figure 6 was constructed and analyzed. The single cell lithium-ion battery was replaced by a desktop supply and a variable electronic load was utilized. The supply was set to a voltage of 4.2V.

Duty Cycle

Continuous mode operation was analyzed at full load current, 250 mA. The output voltage was measured to be 2.90V. Figure 7 is a scope plot of voltage node v_1. Ideally, the voltage at this node would swing from a high value of 4.2V when the switch is on to zero volts when the switch is off. The discrepancy shown here is a result of non-ideal circuit elements. Conduction losses in the switch and diode cause the variations. The measured duty cycle of 78.5% is a direct result of the circuit losses. In the ideal situation, efficiency is 100%. The change in duty cycle directly correlates to the efficiency of the system. Therefore, the efficiency of the system, η, is equal to:

$$\eta = \frac{V_O}{V_S \times Actual\ Duty\ Cycle} \times 100$$

$$\eta = \frac{2.90}{4.20 \times 0.785} \times 100 \approx 88.0\%$$

© 2001 Microchip Technology Inc.

By adding the diode forward voltage drop, the 380 mV swing below ground, to the load voltage in the mathematical model, the predicted duty cycle becomes 78%. Comparing this to the actual measured duty cycle indicates that the majority of the inefficiency is due to the non-ideal characteristics of the diode. As the load current increases, switch conduction losses, inductor core and winding losses, etc. begin to make more of a contribution.

The efficiency of the system, especially at lower output voltages, can be improved by as much as 25% by using a method known as synchronous rectification. Synchronous rectification is accomplished by shunting the diode with a switch that is turned on when the diode should be conducting current. The switch conduction losses should be much less than the diode conduction losses resulting in improved efficiency.

Inductor Current and Voltage

The second scope plot, Figure 8, shows the current and voltage waveforms for the inductor. We will start by examining the voltage. The voltage across the inductor with the switch-on is, ideally, V_s - V_O, or in our application, 1.3V. We have very good correlation. When the switch is off, the voltage should ideally be -V_O. Our measurement indicates -3.4V approximately. The additional -0.4V is, again, due to the non-ideal characteristics of the diode and losses associated with the inductor itself.

The ideal minimum and maximum of the inductor current can be found in Table 1. Ideally, Ia is 235 mA and Ib is 265 mA. Therefore, the peak-to-peak inductor current ripple is 30 mA. The average inductor current is simply equal to the load current, $I_{L(AVG)}$ equals 250 mA. Measured results show a strong correlation. The minimum and maximum measured inductor currents are 230 mA and 270 mA with a peak-to-peak inductor current ripple of 40 mA. The average inductor current was measured as 250.3 mA. These values indicate a strong enough correlation to validate our mathematical models. The errors are a result of parasitics in the circuit including the inductor winding resistance, core loss, and tolerance of the inductance.

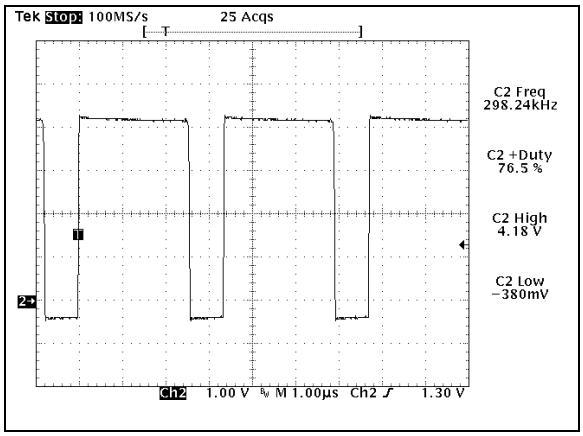

FIGURE 7: *Continuous mode node voltage*

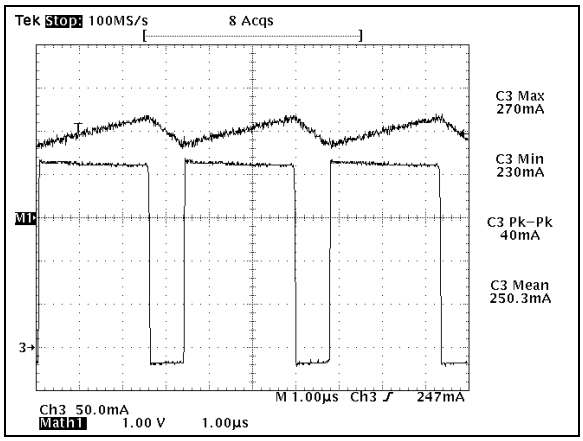

FIGURE 8: *Continuous mode inductor current and voltage*

Load Voltage Ripple

The last performance parameter that we will verify is the load voltage ripple. Ideally, the load voltage ripple was determined to be 15.5 mV peak-to-peak. Figure 9 shows the load voltage ripple along with the inductor current. Remember, we are assuming the AC component of the inductor ripple current flows into the filter capacitor and not into the load.

The measured peak-to-peak load voltage ripple is 21.2 mV. Again, we have good correlation with our mathematical model. Therefore, we can be assured that our assumptions were correct. The discrepancy is, in part, due to the ESR of the filter capacitor. We still have adequate design margin.

© 2001 Microchip Technology Inc.

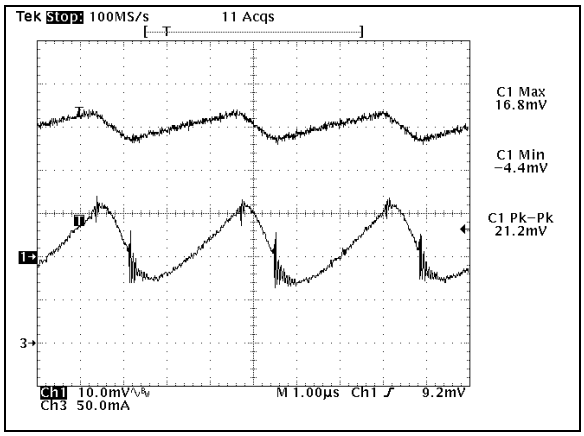

FIGURE 9: *Continuous mode load voltage ripple and inductor current*

Discontinuous Mode Validation

As the load is increased in ohmic value, it is possible that the system will change to discontinuous mode of operation. Solving for the boundary condition between continuous mode and discontinuous mode yields a load current of approximately 15 mA. The transition was measured at approximately 14 mA. The load current was lowered to 5 mA, placing the system well into the discontinuous mode for validation of the mathematical model.

Duty Cycle

Figure 10 is a scope plot of the v_1 node voltage. The ringing present when the inductor has, ideally, transferred all its energy to the load is the result of a small amount of residual energy circulating between the inductor and the capacitance of the switch, diode, and any stray parasitic capacitance. The frequency of the ring is:

$$F_{RING} = \frac{1}{2 \times \pi \times \sqrt{L \times (C_{SW} + C_{D1} + C_{STRAY})}}$$

This is not a sign of instability in the system. The ringing does not cause any harm in the system and trying to suppress it only wastes power.

From Table 1, the ideal duty cycle was calculated to be approximately 0.40. The measured duty cycle is 0.42 showing very good correlation to the model.

Inductor Current and Voltage

The next scope plot, Figure 11, shows the voltage and current waveforms for the inductor. Again, we will start by examining the voltage across the inductor. The voltage across the inductor when the switch is on is the same as in continuous mode, 1.3V. Good correlation is shown. As the inductor transfers energy to the load, the voltage across the inductor is measured as $-(V_O + V_F)$ where V_F represents the forward voltage drop of the catch diode. After the energy has been transferred to the load, the ringing seen previously is present.

The ideal maximum inductor current can be found in Table 1. Ideally, Ib is calculated to be 17.3 mA. The average inductor current is ideally equal to the DC load current. The measured results of 22.8 mA and 5.09 mA, respectively, indicate a strong correlation to the mathematical models.

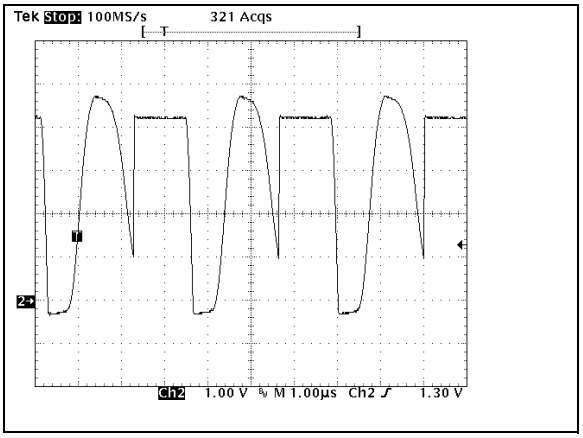

FIGURE 10: *Discontinuous mode note voltage, V_1*

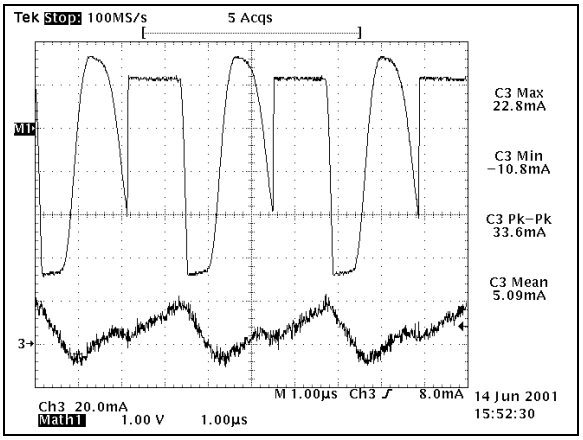

FIGURE 11: *Discontinuous mode inductor current and voltage*

© 2001 Microchip Technology Inc.

Load Voltage Ripple

Figure 12 shows the measured load voltage ripple along with the inductor current.

The measured peak-to-peak load voltage ripple is 20.0 mV. Again, we have adequate design margin. Our assumptions were correct and our ideal mathematical models can be used to predict practical circuit application performance.

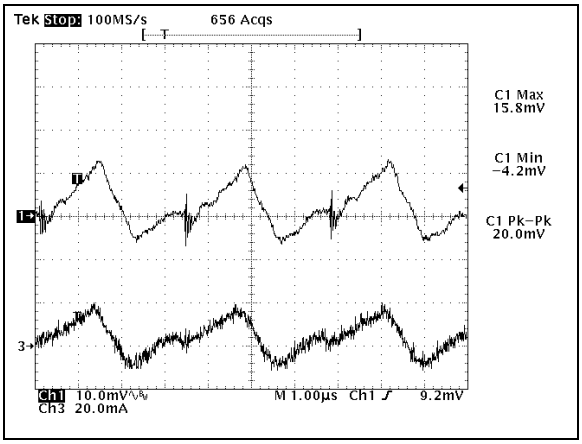

FIGURE 12: *Discontinuous mode load voltage ripple and inductor current*

CONCLUSION

Buck switchmode power convertors are used to step-down a given source voltage to lower magnitude load voltage with the same polarity. Buck switchmode power converts find a home in many portable battery operated applications due to their highly efficient means of power conversion.

A grass roots approach to understanding the buck circuit topology was presented. Mathematical models for an ideal converter were derived and shown to correlate well with a practical design. Parasitic circuit elements can easily be added to the models for a more accurate prediction of circuit performance.

REFERENCES

1. E. Landsman, “A Unifying Derivation of Switching DC-DC Converter Topologies”, in *IEEE Power Electronics Specialists Conference Record* (1979), 239-243.
2. R.P. Severns and G. Bloom, *Modern DC-to-DC Switchmode Power Converter Circuits* (New York: Van Nostrand Reinhold Co., 1985).
3. D.M. Mitchel, *DC-DC Switching Regulator Analysis* (New York: McGraw-Hill, Inc., 1988).
4. R.D. Middlebrook and S. Cuk, “A New Optimum Topology Switching DC-to-DC Converter”, in *IEEE Power Electronics Specialists Conference (PESC) Record* (1977), 160-179.
5. J. Kassakian, M. Schlecht, and G. Verghese, *Principles of Power Electronics* (New York: Addison Wesley Co., 1992).
6. N. Mohan, T. Undeland, and W. Robbins, *Power Electronics: Converters, Applications, and Design* (New York: John Wiley and Sons, Inc., 1989).

© 2001 Microchip Technology Inc.

NOTES:

© 2001 Microchip Technology Inc.

APPENDIX A: CURRENT WAVEFORM APPROXIMATIONS

Note:	For the current waveform approximations, D is the duty cycle defined as the on-time divided by the period

$$D \equiv \frac{t_{ON}}{T}$$

Filter Capacitor RMS Approximations

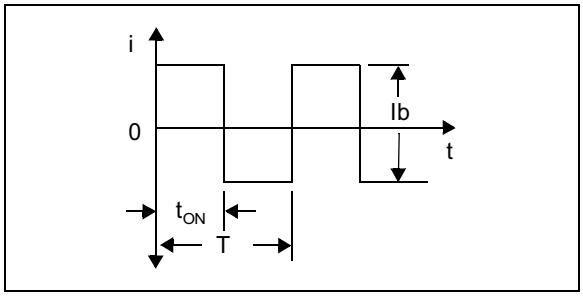

Square wave approximation.

$$i_{(RMS)} = Ib \times \sqrt{D \times (1 - D))}$$

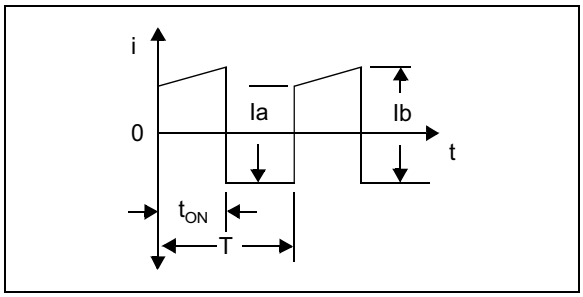

Trapezoidal approximation.

$$i_{(RMS)} = \sqrt{D \times \left[\frac{Ia^2 + Ia \times Ib + Ib^2}{3} - \frac{D}{4} \times (Ia + Ib)^2\right]}$$

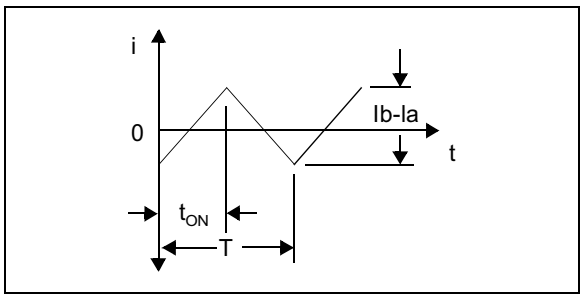

Saw-tooth approximation.

$$i_{(RMS)} = \frac{Ib - Ia}{\sqrt{12}}$$

Switch RMS and Average Approximations

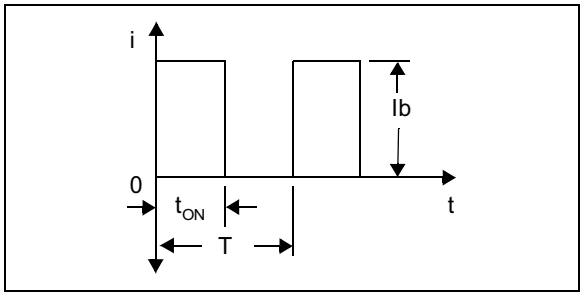

Square wave approximation.

$$i_{(RMS)} = Ib \times \sqrt{D}$$

$$i_{(AVG)} = Ib \times D$$

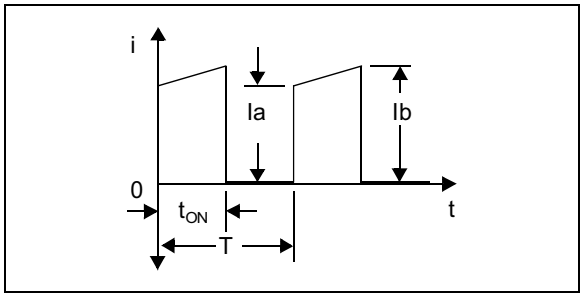

Trapezoidal approximation (continuous mode).

$$i_{(RMS)} = \sqrt{D \times \left[\frac{Ia^2 + Ia \times Ib + Ib^2}{3}\right]}$$

$$i_{(AVG)} = \frac{D \times (Ia + Ib)}{2}$$

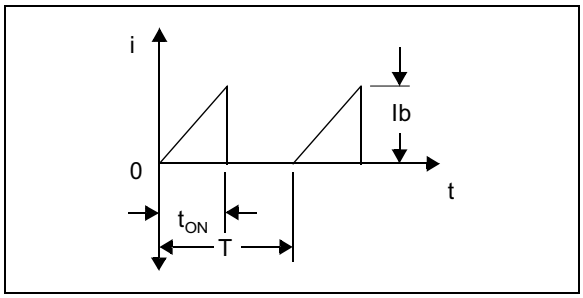

Triangular approximation (discontinuous mode).

$$i_{(RMS)} = Ib \times \sqrt{\frac{D}{3}}$$

$$i_{(AVG)} = \frac{Ib \times D}{2}$$

Diode RMS and Average Approximations

The catch diode currents can be approximated by utilizing the switch approximations. For continuous mode, the duty cycle should be substituted for by (1-D). For discontinuous mode, t_{ON} in the duty cycle equation should be substituted for by the time it takes for the current to ramp to zero, t_2.

NOTES:

© 2001 Microchip Technology Inc.

Information contained in this publication regarding device applications and the like is intended through suggestion only and may be superseded by updates. It is your responsibility to ensure that your application meets with your specifications. No representation or warranty is given and no liability is assumed by Microchip Technology Incorporated with respect to the accuracy or use of such information, or infringement of patents or other intellectual property rights arising from such use or otherwise. Use of Microchip's products as critical components in life support systems is not authorized except with express written approval by Microchip. No licenses are conveyed, implicitly or otherwise, under any intellectual property rights.

Trademarks

The Microchip name and logo, the Microchip logo, PIC, PICmicro, PICMASTER, PICSTART, PRO MATE, KEELOQ, SEEVAL, MPLAB and The Embedded Control Solutions Company are registered trademarks of Microchip Technology Incorporated in the U.S.A. and other countries.

Total Endurance, ICSP, In-Circuit Serial Programming, FilterLab, MXDEV, microID, *Flex*ROM, *fuzzy*LAB, MPASM, MPLINK, MPLIB, PICC, PICDEM, PICDEM.net, ICEPIC, Migratable Memory, FanSense, ECONOMONITOR, Select Mode and microPort are trademarks of Microchip Technology Incorporated in the U.S.A.

Serialized Quick Term Programming (SQTP) is a service mark of Microchip Technology Incorporated in the U.S.A.

All other trademarks mentioned herein are property of their respective companies.

© 2001, Microchip Technology Incorporated, Printed in the U.S.A., All Rights Reserved.

Printed on recycled paper.

DNV Certification, Inc. USA

ANSI-RAB QMS ACCREDITED

DNV MSC The Netherlands Accredited by the RvA

ISO 9001 / QS-9000 REGISTERED FIRM

Microchip received QS-9000 quality system certification for its worldwide headquarters, design and wafer fabrication facilities in Chandler and Tempe, Arizona in July 1999. The Company's quality system processes and procedures are QS-9000 compliant for its PICmicro® 8-bit MCUs, KEELOQ® code hopping devices, Serial EEPROMs and microperipheral products. In addition, Microchip's quality system for the design and manufacture of development systems is ISO 9001 certified.

WORLDWIDE SALES AND SERVICE

AMERICAS

Corporate Office
2355 West Chandler Blvd.
Chandler, AZ 85224-6199
Tel: 480-792-7200 Fax: 480-792-7277
Technical Support: 480-792-7627
Web Address: http://www.microchip.com

Rocky Mountain
2355 West Chandler Blvd.
Chandler, AZ 85224-6199
Tel: 480-792-7966 Fax: 480-792-7456

Atlanta
500 Sugar Mill Road, Suite 200B
Atlanta, GA 30350
Tel: 770-640-0034 Fax: 770-640-0307

Austin - Analog
8303 MoPac Expressway North
Suite A-201
Austin, TX 78759
Tel: 512-345-2030 Fax: 512-345-6085

Boston
2 Lan Drive, Suite 120
Westford, MA 01886
Tel: 978-692-3848 Fax: 978-692-3821

Boston - Analog
Unit A-8-1 Millbrook Tarry Condominium
97 Lowell Road
Concord, MA 01742
Tel: 978-371-6400 Fax: 978-371-0050

Chicago
333 Pierce Road, Suite 180
Itasca, IL 60143
Tel: 630-285-0071 Fax: 630-285-0075

Dallas
4570 Westgrove Drive, Suite 160
Addison, TX 75001
Tel: 972-818-7423 Fax: 972-818-2924

Dayton
Two Prestige Place, Suite 130
Miamisburg, OH 45342
Tel: 937-291-1654 Fax: 937-291-9175

Detroit
Tri-Atria Office Building
32255 Northwestern Highway, Suite 190
Farmington Hills, MI 48334
Tel: 248-538-2250 Fax: 248-538-2260

Los Angeles
18201 Von Karman, Suite 1090
Irvine, CA 92612
Tel: 949-263-1888 Fax: 949-263-1338

New York
150 Motor Parkway, Suite 202
Hauppauge, NY 11788
Tel: 631-273-5305 Fax: 631-273-5335

San Jose
Microchip Technology Inc.
2107 North First Street, Suite 590
San Jose, CA 95131
Tel: 408-436-7950 Fax: 408-436-7955

Toronto
6285 Northam Drive, Suite 108
Mississauga, Ontario L4V 1X5, Canada
Tel: 905-673-0699 Fax: 905-673-6509

ASIA/PACIFIC

Australia
Microchip Technology Australia Pty Ltd
Suite 22, 41 Rawson Street
Epping 2121, NSW
Australia
Tel: 61-2-9868-6733 Fax: 61-2-9868-6755

China - Beijing
Microchip Technology Consulting (Shanghai) Co., Ltd., Beijing Liaison Office
Unit 915
New China Hong Kong Manhattan Bldg.
No. 6 Chaoyangmen Beidajie
Beijing, 100027, No. China
Tel: 86-10-85282100 Fax: 86-10-85282104

China - Chengdu
Microchip Technology Consulting (Shanghai) Co., Ltd., Chengdu Liaison Office
Rm. 2401, Ming Xing Financial Tower
No. 88 TIDU Street
Chengdu 610016, China
Tel: 86-28-6766200 Fax: 86-28-6766599

China - Fuzhou
Microchip Technology Consulting (Shanghai) Co., Ltd., Fuzhou Liaison Office
Rm. 531, North Building
Fujian Foreign Trade Center Hotel
73 Wusi Road
Fuzhou 350001, China
Tel: 86-591-7557563 Fax: 86-591-7557572

China - Shanghai
Microchip Technology Consulting (Shanghai) Co., Ltd.
Room 701, Bldg. B
Far East International Plaza
No. 317 Xian Xia Road
Shanghai, 200051
Tel: 86-21-6275-5700 Fax: 86-21-6275-5060

China - Shenzhen
Microchip Technology Consulting (Shanghai) Co., Ltd., Shenzhen Liaison Office
Rm. 1315, 13/F, Shenzhen Kerry Centre,
Renminnan Lu
Shenzhen 518001, China
Tel: 86-755-2350361 Fax: 86-755-2366086

Hong Kong
Microchip Technology Hongkong Ltd.
Unit 901, Tower 2, Metroplaza
223 Hing Fong Road
Kwai Fong, N.T., Hong Kong
Tel: 852-2401-1200 Fax: 852-2401-3431

India
Microchip Technology Inc.
India Liaison Office
Divyasree Chambers
1 Floor, Wing A (A3/A4)
No. 11, O'Shaugnessey Road
Bangalore, 560 025, India
Tel: 91-80-2290061 Fax: 91-80-2290062

Japan
Microchip Technology Japan K.K.
Benex S-1 6F
3-18-20, Shinyokohama
Kohoku-Ku, Yokohama-shi
Kanagawa, 222-0033, Japan
Tel: 81-45-471- 6166 Fax: 81-45-471-6122

Korea
Microchip Technology Korea
168-1, Youngbo Bldg. 3 Floor
Samsung-Dong, Kangnam-Ku
Seoul, Korea 135-882
Tel: 82-2-554-7200 Fax: 82-2-558-5934

Singapore
Microchip Technology Singapore Pte Ltd.
200 Middle Road
#07-02 Prime Centre
Singapore, 188980
Tel: 65-334-8870 Fax: 65-334-8850

Taiwan
Microchip Technology Taiwan
11F-3, No. 207
Tung Hua North Road
Taipei, 105, Taiwan
Tel: 886-2-2717-7175 Fax: 886-2-2545-0139

EUROPE

Denmark
Microchip Technology Denmark ApS
Regus Business Centre
Lautrup hoj 1-3
Ballerup DK-2750 Denmark
Tel: 45 4420 9895 Fax: 45 4420 9910

France
Arizona Microchip Technology SARL
Parc d'Activite du Moulin de Massy
43 Rue du Saule Trapu
Batiment A - ler Etage
91300 Massy, France
Tel: 33-1-69-53-63-20 Fax: 33-1-69-30-90-79

Germany
Arizona Microchip Technology GmbH
Gustav-Heinemann Ring 125
D-81739 Munich, Germany
Tel: 49-89-627-144 0 Fax: 49-89-627-144-44

Germany - Analog
Lochhamer Strasse 13
D-82152 Martinsried, Germany
Tel: 49-89-895650-0 Fax: 49-89-895650-22

Italy
Arizona Microchip Technology SRL
Centro Direzionale Colleoni
Palazzo Taurus 1 V. Le Colleoni 1
20041 Agrate Brianza
Milan, Italy
Tel: 39-039-65791-1 Fax: 39-039-6899883

United Kingdom
Arizona Microchip Technology Ltd.
505 Eskdale Road
Winnersh Triangle
Wokingham
Berkshire, England RG41 5TU
Tel: 44 118 921 5869 Fax: 44-118 921-5820

06/01/01

© 2001 Microchip Technology Inc.